The Meteoritical Society

Meteoritics & Planetary Science 52, Nr 8, 1669–1682 (2017)
doi: 10.1111/maps.12878

Submillisecond fireball timing using de Bruijn timecodes

Robert M. HOWIE[1*], Jonathan PAXMAN[1], Philip A. BLAND[2], Martin C. TOWNER[2], Eleanor K. SANSOM[2], and Hadrien A. R. DEVILLEPOIX[2]

[1]Department of Mechanical Engineering, Curtin University, Perth, Western Australia 6845, Australia
[2]Department of Applied Geology, Curtin University, Perth, Western Australia 6845, Australia
[*]Corresponding author. E-mail: robert.howie@curtin.edu.au

(Received 29 April 2016; revision accepted 02 March 2017)

Abstract–Long-exposure fireball photographs have been used to systematically record meteoroid trajectories, calculate heliocentric orbits, and determine meteorite fall positions since the mid-20th century. Periodic shuttering is used to determine meteoroid velocity, but up until this point, a separate method of precisely determining the arrival time of a meteoroid was required. We show it is possible to encode precise arrival times directly into the meteor image by driving the periodic shutter according to a particular pattern—a de Bruijn sequence—and eliminate the need for a separate subsystem to record absolute fireball timing. The Desert Fireball Network has implemented this approach using a microcontroller driven electro-optic shutter synchronized with GNSS UTC time to create small, simple, and cost-effective high-precision fireball observatories with submillisecond timing accuracy.

INTRODUCTION

Meteorites provide valuable insight into the formation and history of the solar system and have remained relatively undisturbed since the formation of their parent bodies. There is no shortage of recovered meteorites available for study, but interpreting the results of the physical and chemical analysis is constrained by a lack of knowledge of the precise origins of the samples; this lack of context also limits the conclusions that can be drawn from a single meteorite. The solution is to study planetary materials of known origins. Sample return and rendezvous space missions to asteroids and comets are expensive and high-risk approaches to solving this problem; fireball camera networks which record atmospheric trajectories of bright meteors can provide a cost-effective alternative.

Fireball camera networks traditionally use long-exposure photography from multiple stations to produce a triangulated trajectory with sufficient precision to recover meteorites and calculate heliocentric orbits that can be compared to the orbits of potential parent bodies (Halliday 1973). Long-exposure images are occulted by a periodic shutter in order to determine meteoroid velocity during the observable trajectory (Jacchia and Whipple 1956; Ceplecha 1957). Traditionally, these systems have required separate timing subsystems to record absolute arrival times for orbit calculation (McCrosky and Boeschenstein 1965; Halliday et al. 1978). We present a technique using timecodes constructed from de Bruijn sequences (Flye Sainte-Marie 1894; de Bruijn 1946) to embed the arrival time into the fireball trail image using an electro-optic shutter with no moving parts. This approach enables much smaller, lower power, and more cost-effective fireball cameras than previously possible, and has allowed the rapid deployment of the Desert Fireball Network (DFN) (Bland et al. 2012) in the Australian Outback. The development is significant in that it allows off-the-shelf cameras to be turned into high-precision fireball observatories without the need for additional sensors. The design also significantly simplifies data reduction. The motivation and development will be outlined along with a demonstration of the results produced using the technique to gather all required trajectory data from a single long-exposure image per station.

Using this technique, the Desert Fireball Network has achieved spatial precision of approximately 1 arcminute and submillisecond timing precision at a fraction of the cost of previous observatories. The

technique could also be applied to other areas where high-precision motion-time data are required, including spacecraft, particle image velocimetry, and tracking other objects or phenomena.

FIREBALL CAMERA NETWORKS

Fireball camera networks continuously observe the night sky for rare bright meteors known as fireballs or bolides, which may result in single or multiple meteorite falls. The bright flight or observable luminous trajectory of the fireball (as the meteoroid ablates in the atmosphere) is recorded on a highly accurate imaging device from multiple geographically distinct stations. The meteoroid's trajectory through the Earth's atmosphere is triangulated from these multiple observations in order to determine the estimated fall location and the meteoroid's preatmospheric entry orbit. In addition to the path through the atmosphere, the distributed observatories must also accurately record timing of the trajectory. The relative timing is vital for determining meteoroid velocity and deceleration, which, in combination with the path geometry, allows the estimation of its mass and hence a fall position distribution. The absolute arrival time of the fireball is required to accurately determine the heliocentric orbit of the meteoroid due to the constant orbital motion and rotation of the Earth.

Three large fireball networks were developed in the 1960s and 1970s. The Czechoslovak Fireball Network (now the European Fireball Network) commenced operations with all-sky cameras in 1963 (Ceplecha and Rajchl 1965), shortly followed by the Prairie Meteorite Network in the Midwest United States in 1964 (McCrosky and Boeschenstein 1965) and the Canadian Meteorite Observation and Recovery Project (MORP) in 1971 (Halliday et al. 1978). The Desert Fireball Network (DFN), located in the remote Australian Outback, commenced operation in 2003 with the testing of a large-format film-based observatory based on the recent European Network automated design (Spurný et al. 2006) with modifications for the Australian climate (Bland et al. 2012). The network became operational with three stations in 2005, and a fourth station was added in 2007 (Spurný et al. 2012a). The trial network successfully recovered two meteorites: Bunburra Rockhole (Bland et al. 2009; Spurný et al. 2012a) and Mason Gully (Spurný et al. 2012b; Dyl et al. 2016). This success paved the way for the development and deployment of the first all digital fireball camera network designed for meteorite recovery.

Fireball trajectories must be recorded with high accuracy and precision to ensure meteorites can be located and meteoroid orbits can be meaningfully compared to the orbits of potential parent bodies. Due to the extremely low population density and remoteness of the region, meteorite searches in the Australian Outback are typically conducted by small teams (5–12 persons) on foot, for up to 2 weeks. This places an upper limit on the area of searchable terrain for each predicted meteorite fall (approximately 2–6 km^2), which informs the precision requirements for the network (DFN precision goals for bright flight observations: meteoroid trajectory: $\pm$50 m, triangulation final vector: $\pm$0.05°, mass: 1 order of magnitude). The relative timing along the bright flight trajectory provides the velocity information required to calculate a fall position probability distribution, while the precise absolute arrival time is required for the orbital calculation. Trajectory analysis and mass estimation are performed using the dynamic method detailed in Sansom et al. (2015), giving a robust analysis of the observational and modeling errors involved. After the mass distribution has been estimated, dark flight modeling simulates the meteoroid behavior as it falls to the ground after ablation ceases and it is no longer visible to the camera network; the atmospheric conditions are modeled in the relevant volume from a climate model based on the best available local meteorological data including ground-based measurements and balloon flight data.

Uncertainties in the observed position and velocity of the meteoroid during the trajectory increase the area of the ground search; for this reason, meteor camera networks have previously used large-format film-based cameras to achieve high spatial precision (approximately 1 arcminute, limited by film developing and scanning techniques [Spurný et al. 2006]). The DFN uses high-resolution (36 megapixel), full-frame (24 $\times$ 36 mm) digital sensors with fisheye all-sky lenses to achieve similar spatial precision. The digital observatories are constructed from off-the-shelf components where possible to simplify manufacturing and reduce costs (Howie et al. 2017). They are significantly smaller and easier to manufacture and install than previous designs and integrate with an automated data processing pipeline to greatly reduce the data reduction workload of a large network.

RELATIVE FIREBALL TRAJECTORY TIMING

Relative fireball timing is determined by periodically occulting the sensor or film plane during a long-exposure fireball image. This chops the meteor trail (Fig. 1a) into small segments (Fig. 1b) at a known rate, allowing the calculation of meteoroid velocity throughout the luminous trajectory after triangulation from multiple stations. The first purpose-built fireball observatories in the Czechoslovak network used a

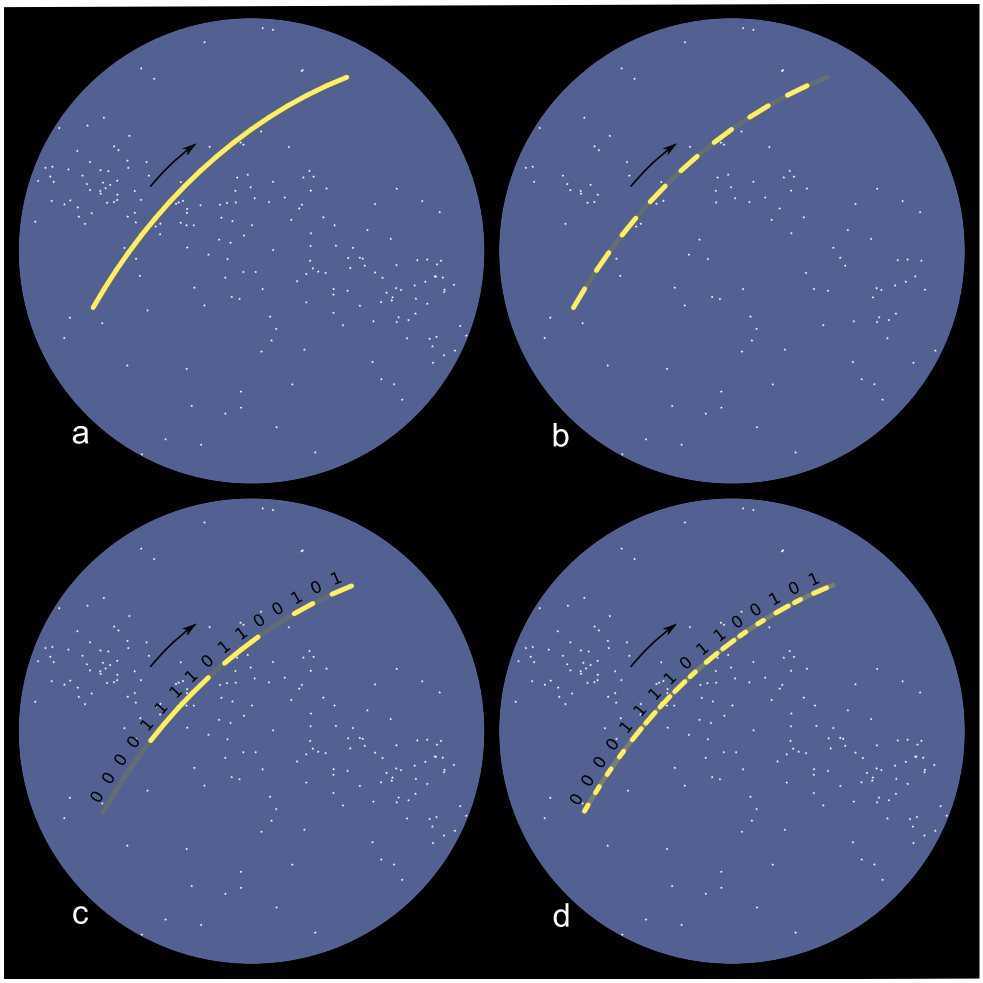

Fig. 1. Long-exposure fireball encoding using a light modulator. a) Long exposure, no encoding. b)Traditional periodic occultation for velocity determination. c) de Bruijn sequence encoded as shutter opacity (0: closed, 1: open). d) de Bruijn sequence encoded as pulse width (0: short, 1: long). (Color figure can be viewed at wileyonlinelibrary.com.)

mechanical rotating shutter to periodically obstruct the film plane similar to previous meteor camera designs (Ceplecha et al. 1959; Ceplecha and Rajchl 1965). The rotational position of the shutter is tightly controlled with respect to time. As the shutter rotates throughout the exposure, the open sectors in the disk create the visible dashes, and the opaque sectors create blanks in the trail where the light path from the fireball to the film plane is obstructed. This relative timing data enables the estimation of fall site distributions but not heliocentric orbits. The Prairie Network replaced the rotating mechanical shutter with a solenoid-controlled switching shutter that moved a lightweight blade in and out of the optical path within the lens (McCrosky and Boeschenstein 1965). This switching shutter operated at 20 cycles per second to produce regular dashes in fireball trails for relative timing similar to the rotating approach. The Canadian MORP network used modified slow-rotating shutters with three different sectors producing four dashes per second, one transparent and two different neutral density filters to allow the imaging of very bright fireballs that would otherwise overexpose the film (Halliday et al. 1978).

Absolute Fireball Trajectory Timing (Arrival Time)

The absolute arrival time of a meteoroid is required in addition to the path and velocity of the meteor's luminous trajectory in order to calculate the meteoroid's preatmospheric orbit due to the constant orbital motion and rotation of the Earth. Because photographs in long-exposure fireball camera networks can be up to one night in length, a method of determining the arrival time of a fireball within the exposure is required. The three large networks took different approaches to the absolute timing problem. The Czechoslovak network

initially relied on chance human observations for arrival times, but was then upgraded to determine absolute timing by comparing images from the fixed fireball cameras with rotating shutters to concurrent images from identical sidereal-guided cameras on equatorial mounts (Ceplecha et al. 1959). The difference in position of the meteor trail image between the two cameras is determined by the position of the guided camera when the meteor arrives. This allows the calculation of the arrival time due to the precise relationship between time of day and the guided camera's position. This method is theoretically simple but relies on very precise movement of the equatorial mount to achieve the specified timing precision of ±5 s (Spurný 1997). The Prairie Network recorded absolute timing by modifying the switching shutter's pattern of operation. A break was extended to denote the beginning of a timing window. Different dashes were omitted in each window by holding the switching shutter closed to indicate which 10.4 s window in the 4 h exposure a fireball appeared (McCrosky and Boeschenstein 1965). A photomultiplier tube (PMT) was also used to timestamp arrivals, but only for meteors brighter than magnitude −4 (fireballs). The MORP observatories were also equipped with a PMT—this time behind interleaved perforated masks to detect motion in the appropriate (angular) velocity range for meteors via an electronic filter circuit. This meteor detector printed the arrival time on the current sheet of film in the camera and then advanced the film to the next frame. The Czechoslovak design (now operating within the European Fireball Network) was updated in the late 1990s with the addition of a PMT to record meteor light curves at a high sample rate and remove the need for guided cameras operating alongside the fixed cameras (Oberst et al. 1998); this Czech design was later automated to reduce the labor demand (Spurný et al. 2006).

Standard video cameras are also used in some fireball networks (Finnish Fireball Network [Gritsevich et al. 2014], Spanish Fireball Network [Trigo-Rodríguez et al. 2005], Polish Fireball Network [Olech et al. 2006], the Croatian Meteor Network [Andreić and Šegon 2010], and others). These video cameras can offer good timing precision, do not require data integration from multiple sensors, and are often used in amateur and collaborative networks where the low per station cost makes them an attractive option. However, the poor spatial resolution offered by systems built around commonly available video cameras paired with all-sky lenses produces significant uncertainty in the fall position and orbit, reducing the likelihood of successful meteorite recovery and the chance of matching an orbit to a potential parent body. Video systems based on expensive high-resolution industrial imaging cameras or using multiple video cameras with rectilinear lenses (such as Cameras for Allsky Meteor Surveillance [CAMS] [Jenniskens et al. 2011]) can achieve similar spatial precision to still cameras. However, the high data rates can make the overall solution complex.

The absolute timing precision required for accurate orbit determination depends on the spatial precision of the observatory. Absolute timing precision of 1 s is sufficient for orbit determination by networks similar to the DFN (high-resolution still cameras with all-sky lenses). More precise timing will not result in more precise orbits due to the spatial uncertainty. The submillisecond timing precision offered by this technique becomes more useful for orbit determination when higher spatial precision instruments such as traditional telescopes and fireball observatories incorporating narrow angle rectilinear lenses are used. The technique can be applied in these higher spatial precision instruments without additional difficulty.

High absolute timing precision is also useful for other purposes aside from orbit determination. The ability to precisely align camera network fireball observations with other timed data sources such as Doppler RADAR (which can provide meteoroid positions at lower altitudes than camera networks) can be beneficial for the recovery of meteorites in more difficult situations. Accurate absolute timing of the data points in fireball images also makes a wider range of triangulation techniques possible because the trajectory data points can be individually triangulated.

A NEW APPROACH

The primary objective during the development of a new fireball observatory for the DFN was to reduce the per station cost in order to deploy the largest network possible on a finite budget while maintaining the precision required for meteorite recovery. The expected number of meteorite dropping fireballs observed by the network per year depends primarily on the network coverage area, and the likelihood of recovery depends on the suitability of the meteorite searching terrain. The primary factors contributing to the high cost of previous designs were the custom large-format film-based imaging system, the precision manufacturing and assembly required to produce the mechanical shutter, and the expensive and complex photomultiplier tube subsystem. The new DFN observatories are based around off-the-shelf consumer digital cameras in order to significantly reduce the per station cost and utilize an automatic data pipeline for triangulation, fall position estimation, and orbit

calculation. After testing a number of camera and lens options, the Nikon D810 (offering high resolution and good low-light noise performance) and Samyang 8 mm f/3.5 II (offering a favorable projection and good value) were selected. A mechanical shutter of the rotating or switching type presents an obstacle to reducing the per observatory cost; the tight manufacturing tolerances and difficult assembly required to implement a precisely controlled mechanical shutter between the lens and sensor plane would significantly contribute to the overall cost of each observatory.

An electro-optic shutter does not require such tight manufacturing tolerances and significantly reduces complexity with no moving parts, resulting in greatly reduced manufacturing and assembly costs. Liquid crystal, polymer-dispersed liquid crystal, and switchable liquid crystal mirror shutter technologies were tested; the liquid crystal (LC) shutter option was selected for its proven track record in long-lasting consumer products (liquid crystal displays), ease of implementation, low cost, and availability. The LC shutter also has the added advantage of global operation, where the transmittance changes across the whole frame with the same timing and hence timing is position independent. This is in contrast to a rotating shutter where the sweeping motion of the rotating shutter across the frame over time must be considered (Ceplecha 1987). The drawback of LC shutters is the limited open state transmittance—approximately 36% for the LC-Tec X-FOS shutters used by the DFN (LC-Tec 2013); this drives the need for good low-light performance from the camera. The LC shutter is mounted between the lens and the sensor plane to periodically obstruct the light path like the mechanical shutters of previous designs, but without moving parts. The shutter must be as thin as possible to minimize focus shift and optical aberrations. The LC shutter is simply mounted over the rear element of the all-sky lens (Fig. 2), and the thin drive wires are routed out through the side of the lens.

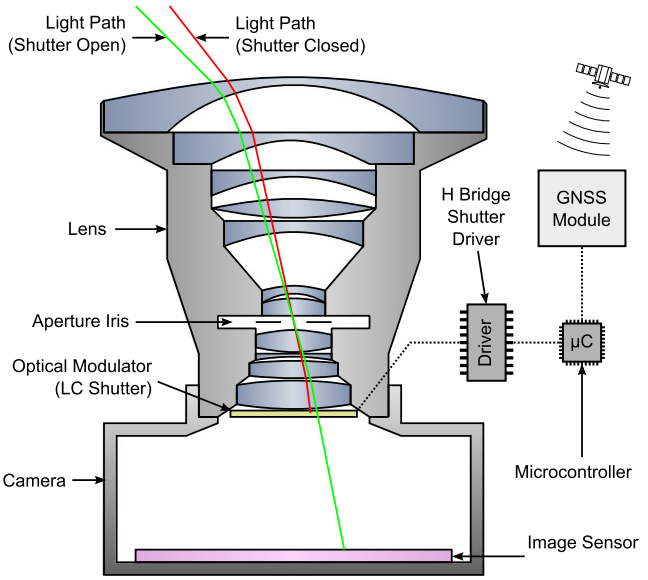

Fig. 2. Imaging system showing all-sky lens, camera, LC shutter, shutter driver, microcontroller, and GNSS receiver. (Color figure can be viewed at wileyonlinelibrary.com.)

A New Technique for Absolute Timing

The previous techniques for determining arrival time in long-exposure fireball images are not ideal for a low-cost fireball camera network deployed in the Australian Outback where the observatories must operate in harsh conditions without manual intervention for periods up to 1 yr. The dust and high winds prevalent in the outback make it difficult and expensive to design and construct precision mechanical systems that operate reliably without frequent maintenance; the dual guided and unguided camera configuration of the original Czechoslovak system was not considered for this reason. The photomultiplier tubes of the recent European network design provide fireball timing along with well-resolved brightness data but are expensive and require high voltage power supplies, complex supporting electronics, a separate optical window or cover, and constant drive voltage adjustments in order to capture a high dynamic range and prevent destruction of the PMT. Processing the brightness curve data is not simple due to the changing drive voltage (affecting gain) and the angle-dependent response of the PMT. Avoiding the added cost and complexity of a separate absolute timing subsystem enables a more cost-effective, smaller, and more power efficient fireball camera. The coded shutter approach of the Prairie Meteorite Network (McCrosky and Boeschenstein 1965) partly achieves this as it records absolute timing in the fireball's trail as it travels across the frame of the long-exposure image, but the precision of the system is too low (within a 10.4 s window) to meet the DFN's objectives for high orbital accuracy.

Time Encoding

Electro-optic shutters make more advanced time encoding straightforward: the devices have fast response times compared to mechanical alternatives and are simple to drive electronically. The flexibility of a microcontroller-driven LC shutter makes it possible to encode absolute timing data (arrival time) by slightly varying the pattern used for relative timing

data (velocity) according to a timecode without requiring any additional hardware. Higher precision than previous attempts at using timecodes—in absolute timing and therefore orbits—is achieved with a constantly changing sequence that does not repeat during the exposure and by synchronizing the operation with highly accurate GNSS time. GNSS or global navigation satellite systems use constellations of satellites (including GPS, GLONASS, QZSS, Galileo, and Compass/BeiDou) to provide users with precise positioning and timing data.

When a meteor or fireball appears, the image of the meteor trail is embedded with a part of this timecode as the meteor moves across the frame, while the LC shutter modulates the light transmittance according to the timecode sequence. The part of the timecode sequence visible in the meteor trail corresponds to the time within the long exposure where the fireball was visible. This records the absolute timing data including the arrival time, and makes the calculation of the heliocentric orbit possible. The recording of the relative and absolute timing data is inherent in the image and does not require the integration of data from multiple subsystems, therefore simplifying the data processing problem.

The ideal timecode should be as long as possible in order to maximize the possible exposure length, but require as few elements visible as possible for time decoding in order to capture the arrival times of short fireballs. While short fireballs are less likely to drop recoverable meteorites, they appear more frequently and are important for the statistical analysis of meteoroid orbits, a secondary goal of the DFN.

A number of different types of sequences were considered as timecodes. The characters in the sequence produce uniquely recognizable image features (e.g., brightness, or dash length—depending on the encoding used); the absolute timing of the trajectory can be determined when the pattern of features visible in the image can be matched with a section of the timecode sequence. The conceptually simplest is a counter sequence with each digit encoded as a different shutter opacity (the first approach in Table 1). This type of sequence is not optimal because the start of each subsequence is not defined and the number of elements that must be visible to decode the unique arrival time varies throughout the sequence. An alternate encoding with a character reserved to define the start of each subsequence could be used (the second approach in Table 1), but this is an inefficient usage of a character in the sequence alphabet that could otherwise be used to extend the sequence. A longer sequence allows a longer exposure on the fireball observatory; this extends the camera lifetime and reduces the amount of data collected per night resulting in longer periods between visits for maintenance and drive changes.

Table 1. A simplistic comparison of three timecode approaches using the three character alphabet {0,1,2}. Each sequence requires three elements to be known for the unique position within the sequence (time within the timecode) to be discovered (for all positions in the sequence).

Approach	Resulting sequence	Sequence length
Counter sequence	000102101112202122	18
Counter sequence with reserved start character	200201210211	12
de Bruijn sequence	000222122021121020120011101	27

The optimal solution for this type of problem is a sequence that includes every subsequence exactly once for a given subsequence length (the third approach in Table 1). This type of sequence is known as a full-length cycle or de Bruijn sequence (Flye Sainte-Marie 1894; de Bruijn 1946).

DE BRUIJN SEQUENCES

De Bruijn sequences are the shortest cyclic sequences containing all possible subsequences for a given alphabet and subsequence length. Their existence was formally described in Flye Sainte-Marie (1894) and then independently described again several times in the 20th century (de Bruijn 1975). de Bruijn (1946) is the best known of these rediscoveries and the reason they are often referred to as de Bruijn sequences today. Interestingly, their use dates at least as far back as an ancient Sanskrit sutra for memorizing rhythms around 1000 AD (Kak 2000; Stein 2010). As an example, the de Bruijn sequence "00011101" contains all of the eight possible three element subsequences "000," "001," "011," "111," "110," "101," "010," and "100" for the binary alphabet A={0, 1} when considered cyclically (the last three digit subsequence is formed by the last digit and the first two). As a window three elements in length is slid along the cyclical sequence, each subsequence is revealed. In the fireball camera application, the sequence is encoded by the electro-optic shutter over time and the window revealing a particular subsequence is the appearance of a fireball in the frame. The elements visible in the fireball's trail indicate the position in the timecode and therefore the fireball's time of arrival. Subsequences are also referred to as *n*-tuples, where *n* is the subsequence length; de Bruijn sequences are also known as full-length cycles because they contain all possible *n*-tuples.

Given an alphabet $\boldsymbol{A}$ with size k (a k-ary alphabet) and a subsequence length of n, there are number of different particular de Bruijn sequences that satisfy the above criteria. The number $|\boldsymbol{B}|$ distinct sequences $\boldsymbol{B}_i$ for the case $\boldsymbol{B}(k, n)$ can be calculated from de Bruijn's Theorem generalized for k-ary alphabets (Van Aardenne-Ehrenfest and de Bruijn 1951) (Equation 1).

$$|\boldsymbol{B}| = \frac{(k!)^{k^{n-1}}}{k^n} \tag{1}$$

For many applications such as meteor trajectory encoding, it is not important to know all of these sequences, or even the number of distinct sequences. What is required, however, is the ability to procedurally generate at least one of these sequences for all relevant cases of n and k. There are various algorithms for developing de Bruijn sequences, many of which are discussed in Fredricksen (1982) and Mitchell et al. (1996). Memory usage and computation speed of these algorithms are of interest to users in the fields of communication and genetics where sequences can be billions of elements long (Compeau et al. 2011); these factors are unimportant for fireball cameras where only relatively short sequences (several hundred elements in length) are required for encoding meteor trajectory data. The length of the de Bruijn sequences N depends on the subsequence length n and the alphabet size k (Equation 2).

$$N = k^n \tag{2}$$

This length refers to the size of the cyclic sequence where the subsequence beginning with the last element in the sequence is completed by the first n-1 elements. The number of possible sequences increases rapidly as the alphabet size or subsequence lengths increase. There are 24 possible distinct sequences of nine elements in length for $\boldsymbol{B}(k = 3, n = 2)$, but this increases to 373,248 distinct sequences of 27 elements in length for the case $\boldsymbol{B}(k = 3, n = 3)$.

de Bruijn Sequence Generation

A repeatable method of generating de Bruijn sequences is required to implement the encoding on the observatory and the decoding in the image processing pipeline; one of the simpler ways to construct a de Bruijn sequence is the prefer high method which is a generalization of the prefer one method for binary alphabets detailed in Fredricksen (1982). The construction starts with n zeros. Then the highest number in the alphabet (k-1) is inserted unless this would produce an n-tuple already present in the sequence. In this case, the next highest element is tried and the process continues until the sequence is complete. An implementation of this algorithm is presented above in pseudocode.

```
algorithm prefer high de Bruijn sequence generation:
  set n to sequence length
  set k to alphabet size
  make empty list sequence
  for n times:
    append 0 to sequence
  while length of sequence is less than or equal to k^n:
    set i to k-1
    set element added to false
    while element added is false:
      set test n-tuple to last n-1 elements of sequence concatenated with i
      if sequence does not contain test n-tuple:
        append i to sequence
        set element added to true
      else:
        decrement i by 1
  return sequence
```

This method is simple to implement, but there is no methodical way to know where a particular subsequence appears in the sequence without generating it and performing a search. This requirement can become quite computationally expensive for longer sequences. Others have focused on constructing decodable de Bruijn sequences that do not require this brute force approach (Mitchell et al. 1996), but this is unnecessary for meteor time encoding as the short sequences only take fractions of a second to generate and search.

SEQUENCE ENCODING

The sequence encoding defines the way in which the de Bruijn sequence is used to modulate the transmittance of the electro-optic shutter. The state of the shutter is changed over time according to the elements of the sequence; two options were tested on the DFN observatories. In the initial method, the sequence was encoded in shutter opacity. A "0" was encoded with a fully darkened shutter, a "1" was encoded with a partially opened shutter, and a "2" was encoded with a fully opened shutter. This encoding is simple to implement, even with an alphabet of arbitrary size, but has two main drawbacks for meteor trajectory timing. First, it can be difficult to distinguish between the fully and partially open shutter states for fireballs with rapidly changing brightness due to fragmentation. This

is especially true when examining dim fireballs at the edges of all-sky images where resolution is decreased and optical aberrations are more prevalent. The problem can be alleviated by only using a binary alphabet with the shutter open and closed, producing the encoding as in Fig. 1c. The second problem with the opacity encoding approach is the ambiguity when velocity is uncertain. If only a few sequence elements are visible, it can be impossible to decode the sequence because the dash length is unknown. For example, the subsequence "222000111," which would be encoded as a bright dash, a blank of equal length, and then a dim dash of equal length, appears identical to the subsequences "220011" and "201" if the velocity is completely unknown. A related problem is that the data points from the dash endpoints are not generated at a consistent rate. Areas of the de Bruijn sequence where elements are repeated have a lower data point density than locations where elements are not repeated. This is undesirable and can increase trajectory velocity uncertainty for fireballs arriving at certain times.

A more appropriate encoding method would eliminate this velocity ambiguity and provide data points at a constant rate. Encoding the sequence elements as pulse width instead of opacity (Fig. 1d) is simple with the flexible shutter driver and accomplishes this goal. The encoding has only been implemented for a binary alphabet for ease of decoding with high sequence rates, but could be generalized to larger alphabets. A "0" is encoded with a short dash length and a "1" is encoded with a longer dash length; there is no velocity ambiguity and data points have a consistent density throughout the sequence. Pulse width encoding also clearly shows the direction of a fireball even when only a couple of dashes are visible.

Sequence Parameters for Fireball Observation

The appropriate parameters of the de Bruijn sequence depend on the imaging configuration and target meteor characteristics. The appropriate sequence rate (in elements per second) depends on the expected velocity of the target meteor and the amount of halation or blurring caused by optical aberrations in the imaging system and meteor trail length. If the sequence rate is too high for a particular scenario, the elements (dashes) in the sequence will smear together making the decoding difficult or impossible. A sequence rate near the upper limit is desirable to provide as many trajectory timing data points as possible and therefore, a more accurate meteoroid mass estimation—using the dynamic method (Sansom et al. 2015)—and fall position distribution. Faster meteors can be imaged with a higher sequence rate than slower meteors because each dash and blank of the meteor trail is projected across more pixels on the sensor making it easier to discern between the individual segments. The DFN is currently optimized for slower fireballs operating at a rate of 10 sequence elements per second with 8 mm all-sky lenses and 36 megapixel full frame (36 × 24 mm) sensors. If the targets of interest are faster, dimmer meteors from a known shower instead of slower, brighter fireballs, the operating parameters could be tuned to produce as many trajectory data points as possible by increasing the sequence rate. The DFN plans to add this capability of switching into an alternate mode of operation during peak periods of known showers in the future.

The sequence duration (t_S) must be greater than the exposure time to avoid duplicating subsequences during the exposure, thereby ensuring a meteor's arrival time during the exposure is unambiguous. The sequence duration depends on the sequence length and the sequence rate (Equation 3); extending the exposure time with a longer sequence duration is desirable due to the corresponding reduction in data rate and storage requirements. If star trails are not a concern, the exposure length is limited by the long-exposure noise performance of the camera.

The minimum time a fireball must be visible for, in order to be decoded, t_{Min} is equal to the subsequence length divided by the sequence rate (Equation 3). t_{Min} has a large impact on t_s and therefore the corresponding data rate of the observatories, all other parameters being equal (Equation 3).

$$t_s = \frac{N}{r_s} = \frac{k^n}{r_s} = \frac{k^{t_{Min} r_s}}{r_s} \tag{3}$$

$$t_{Min} = \frac{n}{r_s} \tag{4}$$

The alphabet size is determined by the number of distinguishable distinct patterns using the chosen encoding and sequence rate. A binary alphabet ($k = 2$) with pulse width modulation at 10 elements per second is used by the DFN ($r_S = 10$). The subsequence length currently used is nine elements ($n = 9$), and hence the minimum decodable meteor duration (t_{Min}) is 0.9 s. This limits the exposure length to 52.0 s. Zeros in the sequence are represented by a short dash where the LC shutter is open for 0.02 s, and ones are represented by a long 0.06 s dash. The starts of the dashes are aligned (every 0.1 s). The DFN observatories take 25 s exposures every 30 s during operation. However, work to extend the open time to 29.0–29.5 s out of 30 is underway. The approximate exposure start time is recorded in the image file by the camera. The de Bruijn

sequence and the camera exposure start every 30 s at the top and bottom of the UTC minute and are precisely (better than 1 ms) synchronized with UTC time through a global navigation satellite system (GNSS) receiver.

Decoding Arrival Time

The DFN currently uses a semiautomated approach to de Bruijn sequence decoding. If the automated event processing routines detect a large fireball appearing simultaneously at multiple stations, the images are downloaded for analysis and decoding. The camera's sequences are synchronized (via the GNSS receivers) so points in the sequence from multiple cameras can be matched. Trajectory triangulation is possible without any knowledge of the de Bruijn sequence.

The search for the subsequence in the overall de Bruijn sequence revealed by each fireball can be performed in a few seconds, either manually or with the assistance of a DFN software tool designed for matching partially obscured de Bruijn sequences. The sequence of long and short dashes are manually translated into the corresponding sequence of "0"s and "1"s; this string is then either found manually within the sequence (usually using a text editor) or fed into the error tolerant search tool. The Hamming distance (Hamming 1950) provides a good metric for finding the location of the subsequence within the complete de Bruijn sequence in a fault tolerant manner. The fault tolerant search is possible because each additional element visible past the required n elements provides a degree of error checking. The current search tool also permits searching for partially obstructed sequences by entering unknown elements. In this situation, the Levenshtein distance (Levenshtein 1966) is used because it also accounts for insertions and deletions unlike the Hamming distance. This is important if the number of elements obstructed is unknown.

Once the subsequence is located within the overall de Bruijn sequence, the absolute timing of the trajectory is simply calculated from the element length t_E, location found in the sequence search, and the dash lengths. The propagation delay due to the operation of the microcontroller and the shutter driver as well as the time response of the LC shutter are also accounted for (these can be determined experimentally and should be less than a millisecond). The approximate time in the image metadata is examined to determine the precisely synchronized sequence start time (hh:mm:00.000 or hh:mm:30.000 UTC) and this is added to the time within the sequence to produce the absolute timing for the trajectory (including the arrival time).

IMPLEMENTATION

The first four prototype long-exposure fireball cameras using LC shutters with de Bruijn timecodes were deployed to The Nullarbor in December 2012. The design has since been revised to expand storage, increase computing power for image processing, and optimize power management. The network now consists of more than 49 observatories covering a double station triangulable area of over 2.5 million square kilometers —approximately one-third of Australia.

The operation of the de Bruijn timecode has been verified in the laboratory with a phototransistor (≈10 μs time response) and a data logging digital oscilloscope. The precision—relative to the GNSS time source—is better than 1 ms, and the time response of the LC shutter is the limiting factor.

This technique, combined with the use of digital off-the-shelf hardware where possible, has enabled the development of smaller, lighter (10×), more cost-effective (20×) fireball observatories for the DFN (compared to the initial film systems) and enabled the rapid roll-out of the digital network. The initial digital DFN observatory for solar-powered operation in remote locations proved the viability of the technique and core imaging system. The observatory hardware is presented in detail in Howie et al. (2017). Recently, an even smaller and lower cost mains powered rooftop variant of the autonomous digital fireball observatory has been developed for powered sites that can be attended more frequently (twice per year).

The LC shutters have proven reliable and long-lasting, and the de Bruijn sequence time encoding has been used to capture precise timing data for over 1,000 fireballs including at least one nine station event and one meteorite recovery with an orbit (Murrili) (Bland et al. 2016). Approximately a dozen of the fireballs observed as of February 2016 have been classified as meteorite dropping by the data processing pipeline, and searches will be conducted for many of these in the future.

Limitations

The technique is validated by the large number of successfully imaged and processed fireballs with timing as well as the recovery of the Murrili meteorite but has a few limitations. Under some conditions, it can be hard to decode the sequence. Extremely bright fireballs pose problems for a few reasons. The all-sky lenses in the DFN's implementation perform best at the image center, but optical aberrations become more prevalent toward the edge of the image. These imperfections can cause the brighter dashes to smear together, becoming

hard to distinguish. Extremely bright fireballs have the potential to saturate large areas of the sensor at the high sensitivity settings used to image as much of the fading fireball at the end of its luminous trajectory as possible. This obstacle is present in all imaging systems because of the limited dynamic range of digital sensors and film. This problem will be reduced as higher dynamic range sensors are developed and become available. The other limitation with respect to bright fireballs is the transmittance of the shutter in the closed state. The shutter still allows a small percentage of the incoming light (approximately 0.45%) (LC-Tec 2013) through in the closed state. This light bleed can complicate the time decoding of extremely bright fireballs. Fireball tails and fragmentation also present some problems for the implementation of timecodes in long-exposure images. Very long tails can be visible in the space where the image of the fireball head was darkened by the shutter. This is the downside of this sort of spatial-time encoding used for the de Bruijn sequence time encoding and previous long-exposure meteor camera techniques (rotating and switching shutters). If the tail is long enough to completely cover the break between dashes, decoding timing can become difficult or impossible. Video networks solve this timing problem by eliminating the long exposures, but compromise on spatial precision. The precise positioning of the data points can be degraded by the tail effect in both video and photographic networks if a simple data point extraction algorithm (such as finding the centroid) is used. The tail has the effect of dragging the apparent data point away from the true point at the head of the fireball.

Another limitation inherent in any long exposure system employing a periodic shutter is that part of the fireball trail is obscured. Flares due to fragmentation and other variations in brightness during breaks where the shutter is closed can be missed. For this reason, radiometers such as PMTs are used where the mass estimation is performed using the photometric method (Gritsevich and Koschny 2011). The dynamic method used as part of the DFN's data pipeline (Sansom et al. 2016) incorporates these fragmentation events by the corresponding observed deceleration, but most DFN observatories also employ a video camera so that data can be collected on these fragmentation events more directly.

Fragmentation performance of the de Bruijn sequence time encoding has been better than expected. While fragmentation of the fireball into multiple heads does make the (currently manual) point picking process take longer, it is possible to distinguish between the main mass and smaller fragments in almost every case. These fragments have been processed separately on a number of fireballs to produce separate fall position estimates for the fragments and main mass.

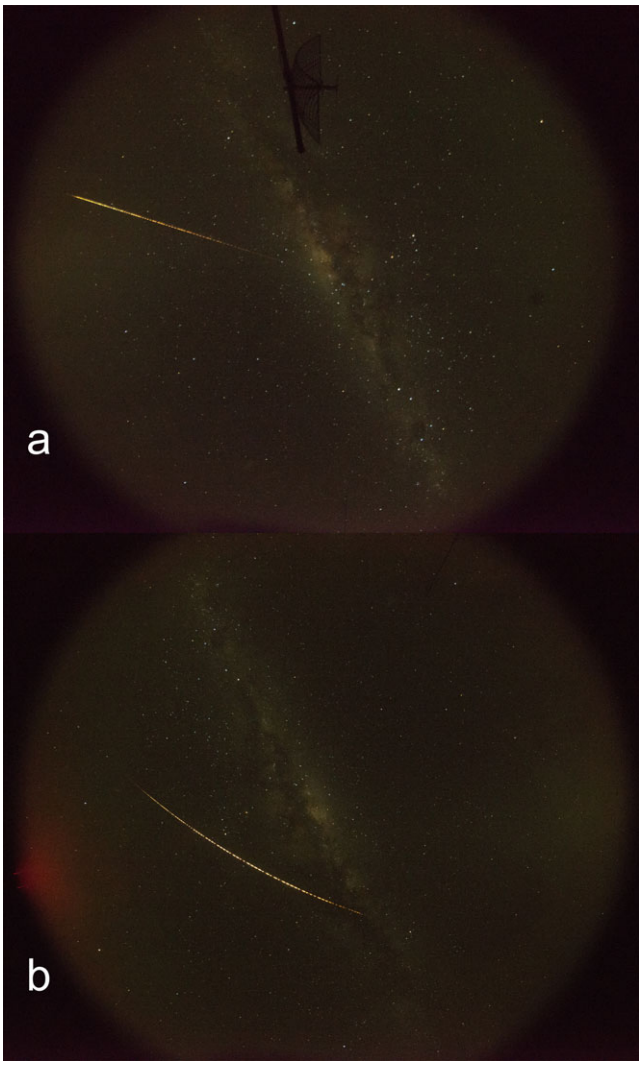

Fig. 3. DN150417_01 Fireball seen from DFN observatories at Kybo (a) and Forrest (b). (Color figure can be viewed at wileyonlinelibrary.com.)

These limitations are present in all long-exposure meteor camera systems that interrupt the meteor image for relative or absolute timing. In its current state, the approach is suitable for imaging the vast majority of meteorite dropping fireballs, but as lens designs and sensor technologies improve (with reduced optical aberrations and increased sensor dynamic range), the results for very faint and extremely bright fireballs will only improve.

RESULTS IN PRACTICE: DN150417_01

On April 17, 2015, a fireball event in the upper atmosphere above the West Australian Nullarbor

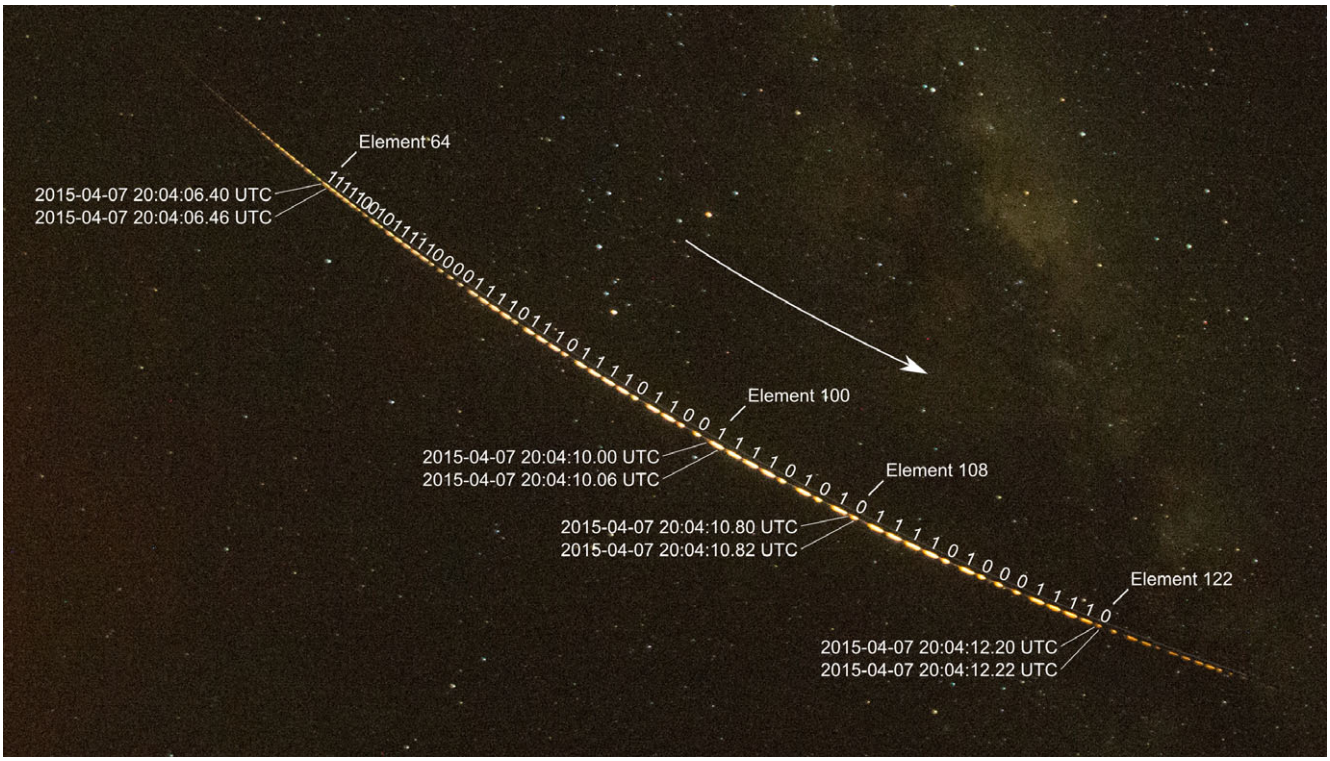

Fig. 4. DN150417_01 fireball observed from Forrest observatory showing de Bruijn sequence encoded timing (alphabet size $k = 2$, subsequence length $n = 9$, rate $r_s = 10$ elements per second, generated using the prefer high method). Element 0 is at 2015-04-07 20:04.00 UTC. Sequence: 000000000111111111011111110011111101011111000111101101111101001**111110010111110000111101110111001**10111110010011110001011110000011101110011101101011101100011101011011010100111010010111010000111001100111001010111001000111000110111000100111000010111000000011011 01101001101100101101100001110101100110101010111010100011010010011010001011010000011001100011001010011001001011001100001101011001101010101101010001101001001101000101101000001100110001100101001100100 00110000100110000010110000000101010100101010000101001000101000100100 10000001001001000001000100001 (labeled elements in bold). (Color figure can be viewed at wileyonlinelibrary.com.)

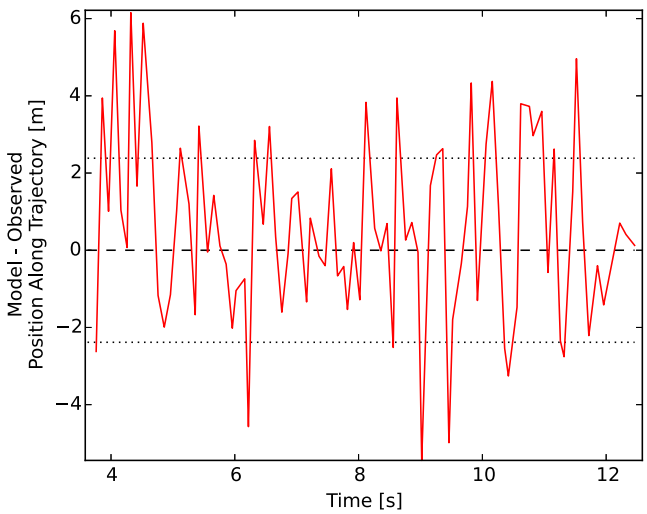

Fig. 5. Observed versus modeled position residuals along the straight-line trajectory, dashed lines indicate $\pm 1\sigma$ range. (Color figure can be viewed at wileyonlinelibrary.com.)

designated as DN150417_01 was recorded by five DFN observatories and is presented here to demonstrate the use of de Bruijn timecodes in long-exposure fireball photography; the object became visible to the camera network at UTC20:04:04.3270 ± 0.0006 s traveling eastwards and remained observable for 10.4590 ± 0.0007 s without visible flares or fragmentation until observable ablation ceased at UTC20:04:14.7864 ± 0.0001 s.

The best observations were made from the closest DFN cameras at Kybo (Fig. 3a) and Forrest (Fig. 3b), adjacent settlements located along the Trans-Australian Railway. The sites are separated by nearly 150 km and each have a permanent population of approximately two persons (giving an indication of the population density in the coverage area of the DFN). The trajectory triangulation was performed using four of the five observations (Kybo, Forrest, Deakin North, and Kanandah). Hughes was excluded because distant and low to the horizon observations result in reduced

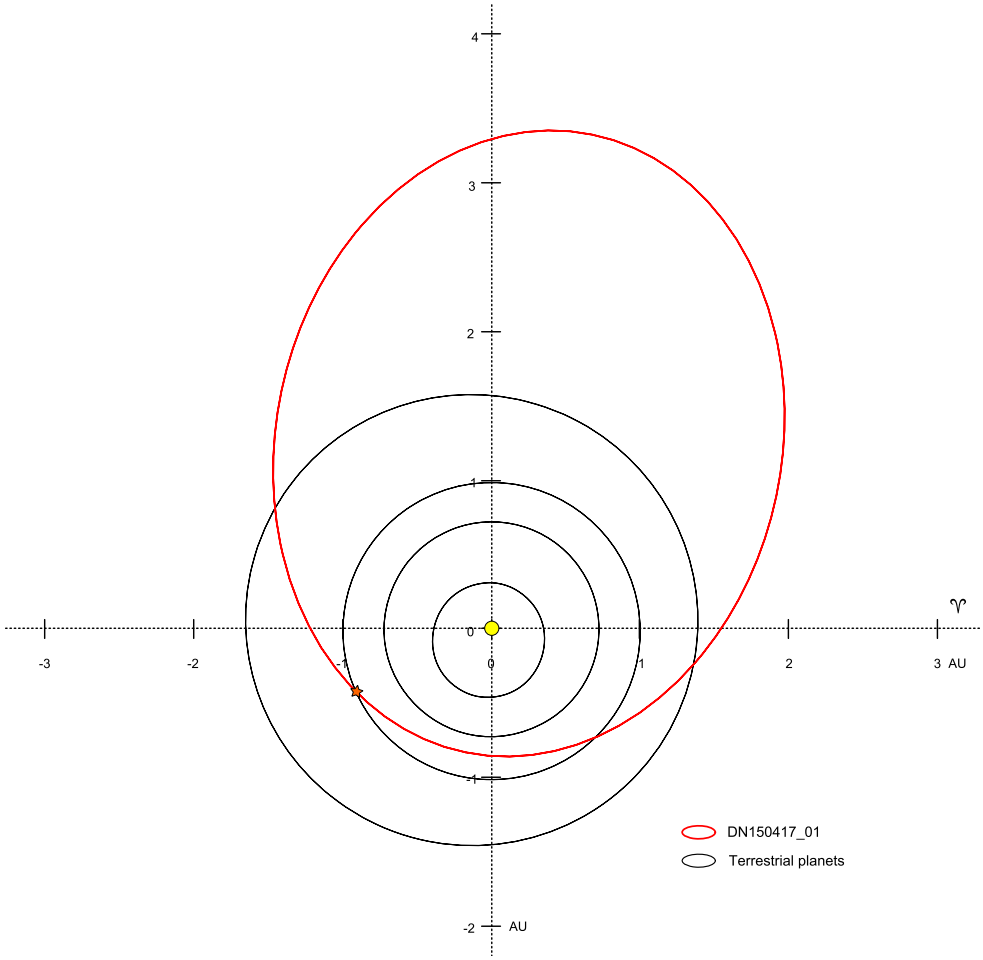

Fig. 6. Heliocentric orbit for DN_15041701 meteoroid. (Color figure can be viewed at wileyonlinelibrary.com.)

precision (compared to the closer cameras with better triangulation geometry).

Trajectory timing was recorded by the DFN observatories using the de Bruijn timecode approach. The timing embedded by the GNSS synchronized LC shutter into the Forrest observatory image is illustrated in Fig. 4. The trajectory was triangulated according to the straight least squares method (Borovička 1990) and analyzed using the dynamic method described previously (Sansom et al. 2015), which uses the observations to estimate the position, mass, and velocity of a meteoroid while statistically constraining the uncertainties in these parameters introduced by observation and dynamic model errors. The object appeared at a height of 85.80 ± 0.05 km at 126.7166 ± 0.0003°E 31.02550 ± 0.00022°S (WSG 84) with an initial velocity of 17.98 ± 0.07 km s^{-1} and an entry angle of 15.14 ± 0.05° from the horizontal. The object gradually decelerated over the 143.31 ± 0.01 km luminous trajectory, which ceased at a height of 45.70 ± 0.03 km at 128.23950 ± 0.00017°E 30.57766 ± 0.00015°S (WSG 84) and a final velocity of 4.4 ± 0.7 km s^{-1}. The trajectory analysis indicates the fireball event was the result of a small meteoroid with an initial mass of 32 ± 4 kg entering the atmosphere at a shallow angle before completely burning up. The position residuals from the trajectory analysis (Fig. 5) show a good fit between the observations and the dynamic model.

The heliocentric orbit (Fig. 6) was calculated from the initial entry vector using a numerical propagation technique that accounts for perturbations caused by a number of small solar system bodies. The eccentric and slightly inclined orbit has its aphelion inside the Main Belt and its perihelion between the orbits of Earth and Venus (e = 0.5992, a = 2.132 AU, i = 6.960°, Ω = 207.59011°, ω=51.06° J2000).

These data were entirely derived from the four images taken by the DFN observatories with the relative timing for trajectory analysis and the absolute timing for orbit calculation embedded by the de Briujn sequence timecode.

FUTURE WORK

Extraction of fireball data points from images with timing is currently performed manually with the assistance of a custom software tool. It is the only time-consuming step remaining in the DFN's data pipeline that has not been automated. The development of image-processing software to handle this task is a priority. The problem is simple in the ideal case (a fast-moving fireball in the center of the lens with no blown highlights and minimal fragmentation and tail), but significantly more difficult when the fireball is partially obstructed, close to the extreme edge of the image, or contains bright flares. Once the data points can be precisely located automatically in most conditions, the automatic decoding of de Bruijn sequence timing is simple. Newer trajectory triangulation techniques that take advantage of the fact that each data point along the trajectory can be independently triangulated are currently being developed and will be tested against more traditional techniques that make the straight line assumption.

Other aspects warranting further study include the viability of larger ternary and quaternary alphabets (three or four different pulse lengths), higher sequence rates for imaging known meteor showers, real-time adjustment of the LC shutter in response to very bright fireballs to prevent sensor saturation, and the testing of other higher transmittance electro-optic shutter technologies. The method may also be useful in other fields where precise motion-time data are required such as spacecraft, fluid dynamics, and high speed tracking of other (nonmeteoroid) objects.

Acknowledgments—The authors thank Robert Yuncken for discussions in the development of this work. This research was supported by the Australian Research Council through the Australian Laureate Fellowships scheme and receives institutional support from Curtin University. The authors also thank Maria Gritsevich and Lukáš Shrbený for their constructive feedback which has significantly improved the quality of this manuscript. The authors have no conflicts of interest to declare.

Editorial Handling—Dr. Josep M. Trigo-Rodríguez

REFERENCES

Andreić Ž. and Šegon D. 2010. The first year of Croatian Meteor Network. In *Proceedings of the International Meteor Conference 27th IMC, Sachticka, Slovakia, 2008* pp. 16–23.

Bland P. A., Bland P. A., Spurny P., Towner M. C., Bevan A. W., Singleton A. T., Bottke W. F. Jr ., Greenwood R. C., Chesley S. R., Shrbeny L., Borovicka J., Ceplecha Z., McClafferty T. P., Vaughan D., Benedix G. K., Deacon G., Howard K. T., Franchi I. A., and Hough R. M. 2009. An anomalous basaltic meteorite from the innermost Main Belt. *Science* 325:1525–1527.

Bland P., Spurny P., Bevan A. W. R., Howard K. T., Towner M. C., Benedix G. K., Greenwood R. C., Shrbený L., Franchi I. A., Deacon G., Borovicka J., Ceplecha Z., Vaughan D., and Hough R. M. 2012. The Australian Desert Fireball Network: A new era for planetary science. *Australian Journal of Earth Sciences* 59:177–187.

Bland P. A., Towner M. C., Sansom E. K., Devillepoix H., Howie R. M., Paxman J. P., Cupak M., Benedix G. K., Cox M. A., Jansen-Sturgeon T., Stuart D., and Strangway D. 2016. Fall and recovery of the Murrili meteorite, and an update on the desert fireball network (abstract #6265). *Meteoritics & Planetary Science* 51:A144–A692.

Borovička J. 1990. The comparison of two methods of determining meteor trajectories from photographs. *Bulletin of the Astronomical Institutes of Czechoslovakia* 41:391–396.

de Bruijn N. G. 1946. A combinatorial problem. *Koninklijke Nederlandse Akademie v. Wetenschappen* 49:758–764.

de Bruijn N. G. 1975. Acknowledgement of priority to C. Flye Sainte-Marie on the counting of circular arrangements of 2n zeros and ones that show each n-letter word exactly once. *EUT report. WSK, Deptartment of Mathematics and Computing Science, Volume 75-WSK-06*. Eindhoven, the Netherlands: Technische Hogeschool Eindhoven.

Ceplecha Z. 1957. Photographic Geminids 1955. *Bulletin of the Astronomical Institutes of Czechoslovakia* 8:51.

Ceplecha Z. 1987. Geometric, dynamic, orbital and photometric data on meteoroids from photographic fireball networks. *Bulletin of the Astronomical Institutes of Czechoslovakia* 38:222–234.

Ceplecha Z. and Rajchl J. 1965. Programme of fireball photography in Czechoslovakia. *Bulletin of the Astronomical Institutes of Czechoslovakia* 16:15.

Ceplecha Z., Rajchl J., and Sehnal L. 1959. Complete data on bright meteor 15761. *Bulletin of the Astronomical Institutes of Czechoslovakia* 10:204.

Compeau P. E., Pevzner P. A., and Tesler G. 2011. How to apply de Bruijn graphs to genome assembly. *Nature Biotechnology* 29:987–991.

Dyl K. A., Benedix G. K., Bland P. A., Friedrich J. M., Spurný P., Towner M. C., O'Keefe M. C., Howard K., Greenwood R., Macke R. J., Britt D. T., Halfpenny A., Thostenson J. O., Rudolph Rebecca A., Rivers M. L., and Bevan A. W. R. 2016. Characterization of Mason Gully (H5): The second recovered fall from the Desert Fireball Network. *Meteoritics & Planetary Science* 51:596–613.

Flye Sainte-Marie C. 1894. Solution to question nr. 48. *L'intermédiaire des Mathématiciens* 1:107–110.

Fredricksen H. 1982. A survey of full length nonlinear shift register cycle algorithms. *SIAM Review* 24:195–221.

Gritsevich M. and Koschny D. 2011. Constraining the luminous efficiency of meteors. *Icarus* 212:877–884.

Gritsevich M. Lyytinen E., Moilanen J., Kohout T., Dmitriev V., Lupovka V., Midtskogen V., Kruglikov N., Ischenko A., Yakovlev G., Grokhovsky V., Haloda J., Halodova P., Peltoniemi J., Aikkila A., Taavitsainen A., Lauanne J., Pekkola M., Kokko P., Lahtinen P., and Larionov M. 2014. First meteorite recovery based on observations by the Finnish Fireball Network. In *Proceedings of the*

International Meteor Conference, Giron, France, 18-21 September 2014, edited by Rault J.-L. and Roggemans P. International Meteor Organization.

Halliday I. 1973. Photographic fireball networks. In *Evolutionary and physical properties of meteoroids: The proceedings of the International Astronomical Union's colloquium # 13, held at the State University of New York, Albany, NY, on June 14-17, 1971*, edited by Hemenway C. L., Millman P. M. K., Cook A. F., and Union I. A. Washington, D.C.: Scientific and Technical Information Office, National Aeronautics and Space Administration. p. 1.

Halliday I., Blackwell A., and Griffin A. 1978. The Innisfree meteorite and the Canadian camera network. *Journal of the Royal Astronomical Society of Canada* 72:15–39.

Hamming R. W. 1950. Error detecting and error correcting codes. *Bell System Technical Journal* 29:147–160.

Howie R. M., Paxman J., Bland P. A., Towner M. C., Cupak M., Sansom E. K., and Devillepoix H. A. R. 2017. How to build a continental scale fireball camera network. *Experimental Astronomy*, doi:10.1007/s10686-017-9532-7

Jacchia L. G. and Whipple F. L. 1956. The Harvard photographic meteor programme. *Vistas in Astronomy* 2:982–994.

Jenniskens P., Gural P. S., Dynneson L., Grigsby B. J., Newman K. E., Borden M., Koop M., and Holman D. 2011. CAMS: Cameras for Allsky Meteor Surveillance to establish minor meteor showers. *Icarus* 216:40–61.

Kak S. 2000. An interesting combinatoric sutra. *Indian Journal of History of Science* 35:123–127.

LC-Tec. 2013. Fast optical shutter series, http://www.lc-tec.com/UserFiles/Products/FOS_Products-130121.pdf.

Levenshtein V. I. 1966. Binary codes capable of correcting deletions, insertions, and reversals. *Soviet Physics Doklady* 10:707–710.

McCrosky R. E. and Boeschenstein H. Jr. 1965. The prairie meteorite network. *Optical Engineering* 3:304127.

Mitchell C. J., Etzion T., and Paterson K. G. 1996. A method for constructing decodable de Bruijn sequences. *IEEE Transactions on Information Theory* 42:1472–1478.

Oberst J., Molau S., Heinlein D., Gritzner C., Schindler M., Spurný P., Ceplecha Z., Rendtel J., and Betlem H. 1998. The "European Fireball Network": Current status and future prospects. *Meteoritics & Planetary Science* 33:49–56.

Olech A., Zoladek P., Wisniewski M., Krasnowski M., Kwinta M., Fajfer T., Fietkiewicz K., Dorosz D., Kowalski L., Olejnik J., Mularczyk K., and Zloczewski K. 2006. Polish fireball network. In *Proceedings of the International Meteor Conference, 24th IMC, Oostmalle, Belgium 2005*, edited by Bastiaens L., Verbert J., Wislez J.-M., and Verbeeck C. International Meteor Organization. pp. 53–62.

Sansom E. K., Bland P., Paxman J., and Towner M. 2015. A novel approach to fireball modeling: The observable and the calculated. *Meteoritics & Planetary Science* 50:1423–1435.

Sansom E., Bland P., Rutten M., Paxman J., and Towner M. 2016. Filtering meteoroid flights using multiple unscented kalman filters. *The Astronomical Journal* 152:148.

Spurný P. 1997. Photographic monitoring of fireballs in Central Europe. In *Optical science, engineering and instrumentation'97*. San Diego, California: International Society for Optics and Photonics. pp. 144–155.

Spurný P., Borovička J., and Shrbený L. 2006. Automation of the Czech part of the European fireball network: Equipment, methods and first results. *Proceedings of the International Astronomical Union* 2:121–130.

Spurný P., Bland P. A., Shrebný L., Borovička J., Ceplecha Z., Singleton A., Bevan A. W. R., Vaughan D., Towner M. C., McClafferty T. P., Toumi R., and Deacon G. 2012a. The Bunburra Rockhole meteorite fall in SW Australia: Fireball trajectory, luminosity, dynamics, orbit, and impact position from photographic and photoelectric records. *Meteoritics & Planetary Science* 47:163–185.

Spurný P., Bland P., Borovička J., Towner M., Shrbený L., Bevan A. W., and Vaughan D. 2012b. The Mason Gully meteorite fall in SW Australia: Fireball trajectory, luminosity, dynamics, orbit and impact position from photographic records (abstract #6369). LPI Contributions 1677. Houston, Texas: Lunar and Planetary Institute.

Stein S. K. 2010. *Mathematics: The man-made universe*. New York: Dover Publications.

Trigo-Rodríguez J., Castro-Tirado A. J., Llorca J., Fabregat J., Martínez V. J., Reglero V., Jelínek M., Kubánek P., Mateo T., and Postigo A. D. U. 2005. The development of the Spanish Fireball Network using a new all-sky CCD system. *Earth, Moon, and Planets* 95:553–567.

Van Aardenne-Ehrenfest T. and de Bruijn N. G. 1951. Circuits and trees in oriented linear graphs. *Simon Stevin: Wis-en Natuurkundig Tijdschrift* 28:203.